Vol. 29 (1998) *ACTA PHYSICA POLONICA B* No 8

EVENT-BY-EVENT ANALYSIS OF HIGH MULTIPLICITY Pb(158 GeV/NUCLEON)–Ag/Br COLLISIONS

M.L. Cherry[b], A. Dąbrowska[a], P. Deines-Jones[b,†], R. Hołyński[a], B.S. Nilsen[b,‡], A. Olszewski[a], M. Szarska[a], A. Trzupek[a], C.J. Waddington[c], J.P. Wefel[b], B. Wilczyńska[a], H. Wilczyński[a], W. Wolter[a], B. Wosiek[a] and K. Woźniak[a]

For the KLM Collaboration

[a] Institute of Nuclear Physics, Kawiory 26A, 30-055 Kraków, Poland
[b] Louisiana State University, Baton Rouge, LA 70803, USA
[c] University of Minnesota, Minneapolis, MN 55455, USA

(Received March 6, 1998)

High multiplicity nucleus-nucleus collisions are studied on an event-by-event basis. Different methods of analysis of individual collision events are presented and their ability to reveal anomalous features of the events is discussed. This study is based on full acceptance measurements of particle production in the interactions of 158 GeV/nucleon Pb with the heavy target nuclei in nuclear emulsion. No events are observed with global characteristics that differ significantly from expectations based on either Monte Carlo simulations, or the characteristics of the entire sample of events. On the other hand, it is shown that systematic analysis of particle density fluctuations in phase space domains of varying size, performed in terms of factorial moments, can be used as an effective triggering for events with large dynamical fluctuations.

PACS numbers: 25.75. Gz, 12.38. Mh, 24.85. +p

1. Introduction

In the quest for a Quark–Gluon Plasma [1] which is the ultimate goal of heavy ion studies foreseen at the RHIC and LHC colliders, great expectations are placed on an event-by-event analysis. It is believed that the characterization of each collision event, in as much detail as possible, should reveal the onset of new phenomena that may occur rarely, only in those few

† Present address: NASA Goddard Space Flight Center, Greenbelt, MD 20771, USA
‡ Present address: Ohio State University, Columbus, OH 43210, USA

individual events in which favorable conditions for the formation of a plasma have been created. It is argued that such an analysis of a single event will be statistically reliable, due to a large number of particles produced in high energy heavy ion central collisions.

The lead ion beam accelerated to an energy of 158 GeV/nucleon at the CERN SPS has already produced events with large multiplicity in collisions of these lead nuclei with heavy stationary target nuclei. In central Pb–Pb collisions more than 2000 hadrons can be produced. Unfortunately, all those experiments studying the symmetric Pb–Pb collisions have a limited acceptance, and only a fraction of the secondary particles is actually recorded (typically a few hundreds per event). The limited acceptance leads not only to a reduction of the number of observed secondaries, but also may distort some event characteristics, such as the particle density fluctuations. In view of this limitation it is worthwhile to attempt an event-by-event analysis of the data obtained from a traditional emulsion experiment, in which a full phase space coverage is ensured, although the available experimental information on particle identification is limited when compared to electronic experiments and, in addition, the total number of measured events is relatively low.

Here we report on the results obtained from the EMU13 emulsion experiment performed by the KLM Collaboration. In this experiment a standard nuclear emulsion stack technique was employed to measure the angular distributions of the charged particles, in central collisions of Pb nuclei with the Ag/Br nuclei in emulsions. The 4π solid angle coverage attained in this detector results in a typical charged particle multiplicity of the order of 1000 per central collision event, and assures that the data are free from biases due to acceptance cuts. In previous papers [2, 3] the properties of multiparticle production and density fluctuations measured for a sample of central Pb–Ag/Br collisions have been presented and compared with the predictions of FRITIOF [4] and VENUS [5] Monte Carlo models. The experimental details on event selections and measurements can be found in those papers.

In this paper we concentrate on the analysis of individual high multiplicity events. It is not immediately obvious what type of analysis can be applied to a single collision event in order to provide statistically meaningful results. Thus the purpose of this study is to demonstrate some possible ways to characterize every event. The applied methods of analysis may allow triggering on different classes of events and identify anomalous features.

To the best of our knowledge so far the only systematic event-by-event analysis was that performed by the NA49 Collaboration for symmetric Pb–Pb collisions [6]. In this analysis the fluctuations in the particle transverse momenta as well as the relative production of kaons and pions was studied. The NA49 approach was based on the definition of some global observable characterizing each event, followed by a statistical analysis of the distribution of this observable in an ensemble of events which was aimed to detect deviations from a reference distribution. The latter have been obtained either by using Monte Carlo simulations or by an event mixing technique. Based on a very large sample of events, no evidence was found for unusual fluctuations in the ratios of kaons to pions, while the fluctuations observed in the particle transverse momenta were shown to be significantly reduced when compared to those present in nucleon–nucleon collisions. This latter effect can be qualitatively explained either as the result of intra-nuclear rescatterings, or as an indication of reaching a thermally equilibrated state in nucleus–nucleus interactions.

In this paper we present the results of an analysis of global event properties (Section 2) for our Pb–Ag/Br data, followed by a more differential study of particle density distributions. In Section 3 the search for inhomogeneities in particle density distributions is described. Section 4 includes the analysis of normalized factorial moments, which allows us to characterize each individual event, and may provide an efficient way to trigger on interesting events. The final section (Section 5) contains the summary and concluding remarks.

2. Global event properties

One possible way to analyze a single collision event is based on the study of some global observable defined in a large region of the available phase space. Such an analysis rests on a comparison of the distribution of this observable, obtained from an ensemble of events, with some reference distribution, *e.g.* such as that predicted by event generators, which follow from the conventional description of nucleus–nucleus collisions. Such a comparison may allow for the detection of events which deviate significantly from the predictions of the reference spectrum. It has to be noted that this type of analysis requires large event samples or large fluctuations.

The simplest global observable that is readily obtainable is the multiplicity of produced particles. In our previous paper [3] we have shown that particle multiplicities measured in central Pb–Ag/Br collisions are satisfactorily reproduced by the FRITIOF and VENUS models, although our analysis of Pb–Pb multiplicities in emulsion chambers [7] has suggested that FRITIOF simulations may under predict the multiplicities in very central collisions. Another global event property is the kaon to pion ratio in each event. As mentioned above, this was studied by the NA49 Collaboration, with no significant excess of events with anomalous relative production of kaons and pions being found. Still another global variable, which is currently the subject of considerable discussion [8], is the ratio of charged to neutral pions. Unusual behavior in the relative production of neutral to charged pions could indicate the creation of a Disoriented Chiral Condensate (DCC) [8]. An analysis of this ratio, performed by the WA98 Collaboration [9] for central Pb–Pb collisions, provided no examples of a DCC.

In the emulsion experiments there is no identification of the produced particles, making a study of the particle ratios, or a search for DCC, impossible. Instead, since the measurements do provide the emission angles of all produced particles, we can study the properties of the particle angular distributions on an event-by-event basis. This produces a global observable that is not available to the other experiments.

2.1. Analysis of particle pseudorapidities

It has been proposed [10] that it would be interesting to study the event-to-event fluctuations of observables which are defined as a sum of particle kinematical variables, such as transverse momentum or rapidity, where the summation runs over all particles produced in a given event. It was shown that by studying the second moment of the distribution of the sum-variable in different classes of events, it may be possible to evaluate the degree of randomization or thermalization characteristic of high multiplicity nucleus–nucleus collisions. The authors [10] defined a measure of fluctuations, Φ, which vanishes in the case of independent particle emission from a single source. On the other hand if the nucleus–nucleus collision is an incoherent superposition of nucleon–nucleon (N–N) interactions, the value of Φ is independent of the number of N–N subprocesses and should be identical to that measured for the nucleon–nucleon system. To satisfy the above features, Φ was defined as:

$$\Phi = \sqrt{\frac{\langle Z^2 \rangle}{\langle N \rangle}} - \sqrt{\langle z^2 \rangle}, \tag{1}$$

where $Z = \sum_{i=1}^{N} z_i$ is calculated for every event, and z_i is the kinematical quantity defined for each of N particles in a given event. In the above definition the brackets, $\langle\ \rangle$, denote averaging over all analyzed events. Thus, $\langle z^2 \rangle$ is the second moment of the inclusive z distribution. For example, in the analysis of particle transverse momenta,p_T, the quantity z_i was defined for each produced particle as

$$z_i = p_{T,i} - \langle p_T \rangle. \tag{2}$$

Such an analysis of particle transverse momenta [6] showed that Φ_{p_T}, measured for central Pb–Pb collisions, was significantly smaller than that predicted by the FRITIOF model, which is based on a pure superposition of N–N collisions. This result may indicate that either particles are produced from a more or less thermally equilibrated state, or that intra-nuclear cascading plays a significant role in destroying the correlations expected in the case of an incoherent superposition of N–N interactions.

We applied a similar procedure to analyze particle pseudorapidities, $\eta = -\ln\tan\theta/2$, where θ is the polar emission angle, measured in our full acceptance Pb–Ag/Br experiment. Thus, for every particle in a given event we define

$$z_i = \eta_i - \langle\eta\rangle\,, \tag{3}$$

where $\langle\eta\rangle$ is the average pseudorapidity of the η distribution measured in the complete sample of central Pb–Ag/Br collisions. The analysis was restricted to η ranging from 0 to 6 (in the laboratory frame) in order to exclude the regions heavily populated by the products of fragmentation of the projectile and target nuclei. The quantities Z and Φ_η were then calculated.

First we check whether Φ_η is independent of the number of contributing N–N processes, by using the FRITIOF event generator. To do this, a minimum bias data set generated by FRITIOF was divided into four subsamples of events with different multiplicities of produced particles, which were characterized by different average numbers of participants, $\langle N_{part}\rangle$. The dependence of Φ_η on the number of nucleon participants is shown in Fig. 1 (stars). One can see that indeed Φ_η is essentially independent of the number of nucleon–nucleon collisions. It is interesting to compare these predictions with those of the VENUS model, in which intra-nuclear rescattering processes are included. The VENUS data are plotted in Fig. 1 as open circles. They agree with the FRITIOF data, except for the most peripheral interactions (the smallest $\langle N_{part}\rangle$), indicating that Φ_η is not affected by rescattering effects.

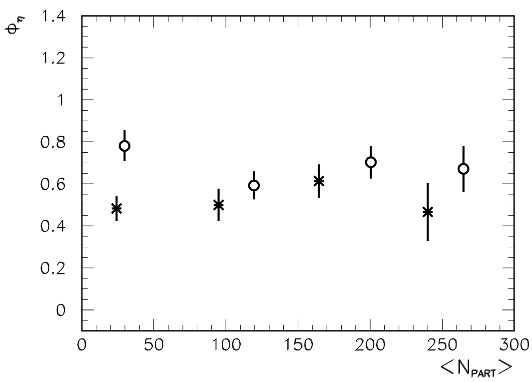

Fig. 1. Fluctuation measure Φ_η as a function of the average number of participants, $\langle N_{part}\rangle$, for FRITIOF (stars) and VENUS (open circles) generated events.

The Φ_η value measured in our sample of 53 central Pb–Ag/Br collisions (9.3 % of all minimum bias events selected as those with highest multiplicities) equals 0.97 ± 0.25 and agrees, within the uncertainties, with Φ_η calculated for the corresponding samples of simulated highest multiplicity events of $\Phi_\eta = 0.74 \pm 0.09$ for VENUS and 0.69 ± 0.10 for FRITIOF. Thus, in contrast to the results of the NA49 analysis of particle transverse momenta, the study of particle pseudorapidities does not show significant deviations from the predictions of Monte Carlo models. This may indicate either, that pseudorapidity distributions are less sensitive to thermalization effects than particle transverse momenta, or that the statistics of the data used in our analysis were not sufficient to reveal discrepancies between the data and the model simulations. It should also be noted that the Φ_η variable, defined in a large phase space region (in our analysis almost in a full phase space), is mostly sensitive to long range correlations. The result $\Phi_\eta > 0$ may thus indicate that some long range correlations (large scale clustering) are present in particle pseudorapidity distributions.

2.2. Roughness of single particle distributions

In this section we compare in detail the η distribution measured in a single collision event to the 'inclusive' distribution, averaged over all analyzed events. We apply a standard χ^2 test to measure deviations of each event distribution from the average. Assume that n_{ik} is the number of particles emitted in the i-th bin of the k-th event, and m_i is the number of particles expected from the averaged distribution. Then for the k-th event we define

$$\chi_k^2 = \sum_{i=1}^{M} (n_{ik} - m_i)^2 / \sigma_{ik}^2 \,, \tag{4}$$

where the sum runs over all bins, M, of width $\delta\eta$ and $m_i = \langle n_{ik} \rangle = \rho_i(\delta\eta)\delta\eta$. For σ_{ik}'s we take statistical errors $\sigma_{ik} = \sqrt{n_{ik}}$. The χ_k^2 defined in Eq. (4) is sensitive to the differences between event multiplicities, N_k, and the average multiplicity of the sample of events, $\langle N \rangle$. We thus use another variable, γ_k^2, which is sensitive only to the shapes of event η distributions:

$$\gamma_k^2 = \sum_{i=1}^{M} \left(n_{ik} - \frac{N_k}{\langle N \rangle} \langle n_{ik} \rangle \right)^2 \Bigg/ n_{ik} . \tag{5}$$

A large value of γ_k^2 would indicate that the hypothesis that n_{ik} multiplicities are drawn from the population represented by $\langle n_{ik} \rangle$ is rather unlikely. In Table I we present the average γ^2 values and the dispersion of γ^2 obtained from the analysis of all measured events as well as from model simulations.

TABLE I

$\langle\gamma^2\rangle$, $\sigma(\gamma^2)$ and confidence levels (CL) for the Pb–Ag/Br data and for the VENUS and FRITIOF simulations.

	$\delta\eta = 0.2$		
	data	VENUS	FRITIOF
$\langle\gamma^2\rangle$	37.7±1.9	36.8±0.8	34.3±0.7
$\sigma(\gamma^2)$	14.1±1.4	10.8±0.6	10.1±0.5
CL	0.18	0.19	0.23
	$\delta\eta = 0.1$		
	data	VENUS	FRITIOF
$\langle\gamma^2\rangle$	71.9±2.1	72.0±1.3	72.9±1.3
$\sigma(\gamma^2)$	15.3±1.5	17.6±0.9	18.3±0.6
CL	0.20	0.20	0.21

The results are presented for two settings of the bin width: $\delta\eta = 0.1$ and $\delta\eta = 0.2$. In each case the corresponding confidence levels (CL) are also quoted. The measured $\langle\gamma^2\rangle$ and $\sigma(\gamma^2)$ are slightly larger than those obtained from simulations only for $\delta\eta = 0.2$. However in all cases, the quoted CL's clearly indicate that we do not observe a statistically significant difference between the event distribution and the average distribution for data as well as for simulations. This observation, however, does not exclude the possibility that the average distribution itself may exhibit some anomalous properties. In fact, we have shown in [3] that this distribution is different from the average distributions predicted by both Monte Carlo models for central Pb–Ag/Br interactions in that it has a smaller width than the FRITIOF distribution but not as small as predicted by the VENUS.

3. Search for high density phase space regions

In the remainder of this paper we attempt to investigate event fluctuations on a more local scale. The purpose of this study is to identify those local regions of phase space with unusually large particle densities *i.e.* those regions where a lot of entropy is confined in a small domain.

3.1. One-dimensional pseudorapidity and azimuthal angle distributions

Densely populated narrow regions in one dimensional distributions are traditionally called spikes. To search for spikes in pseudorapidity distributions we define for the k-th event and for each $\delta\eta$ bin the quantity

$$d_{ik} \equiv \left(n_{ik} - \frac{N_k}{\langle N \rangle} \langle n_{ik} \rangle \right) \Big/ \sigma_{ik}. \tag{6}$$

This quantity measures the local deviation from the average particle density in units of the statistical errors (for which we take, as before, $\sigma_{ik} = \sqrt{n_{ik}}$). Similarly we define d_{ik} quantities for the azimuthal angle (φ) distribution. In Fig. 2 we compare the probability distributions of d_{ik} for the data and the simulations for both η and φ bins. It can be noted that the measured and simulated distributions do not differ significantly, although in the φ bins the tails of the experimental ones are extended to larger d_{ik} values than those for generated events.

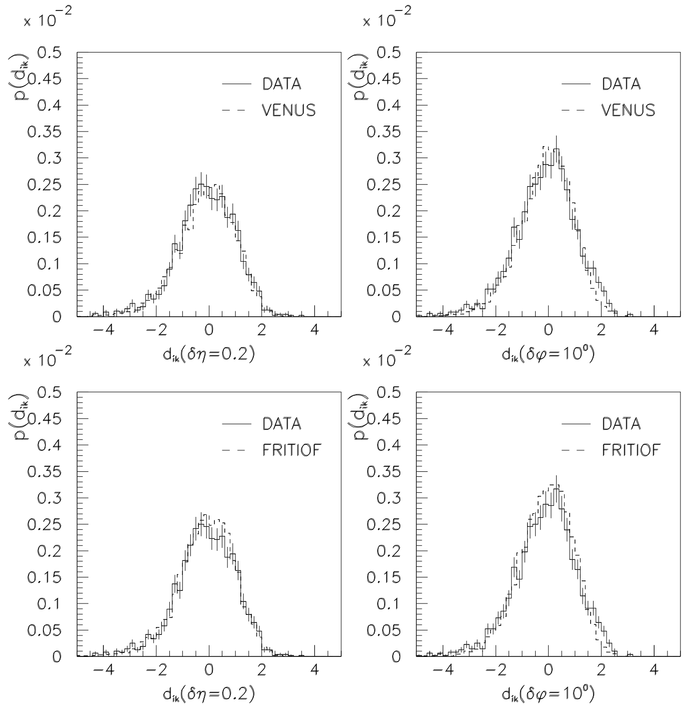

Fig. 2. Comparison of the measured d_{ik} distribution (solid histogram) with the simulations (dashed histograms) in pseudorapidity bins, $\delta\eta = 0.2$ and in the azimuthal angle bins, $\delta\varphi = 10^o$.

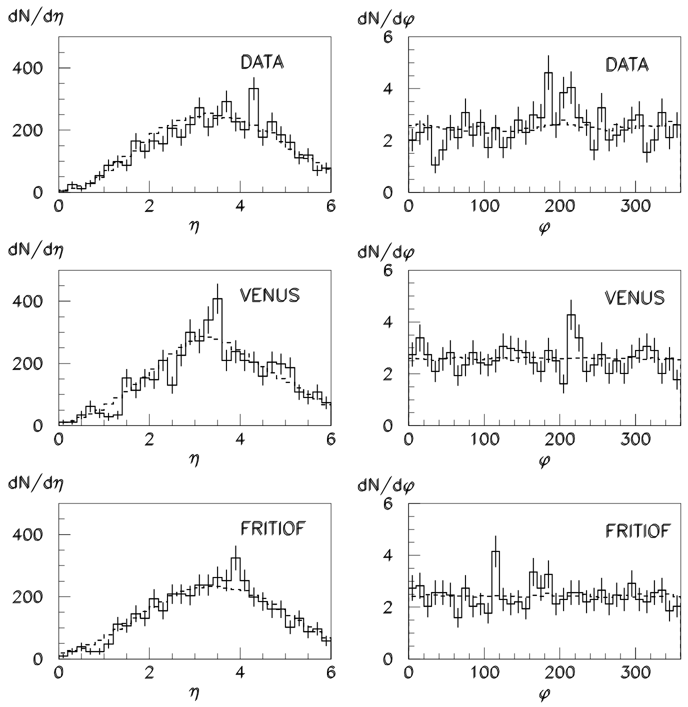

Fig. 3. Events with spikes in η (left-side plots) and φ (right-side plots) distributions. Dashed lines show the distributions averaged over all events.

The interesting , spiky regions (bins) are of course those with largest d_{ik} values. We, thus define as a spike those bins in which d_{ik} is ≥ 2.5. In Table II we list probabilities of occurrence of such spikes and $\langle d_{ik} \rangle$ values for data and models. We see that spikes occur very rarely, but nevertheless they are seen in the data as well as in the simulations,although with a slightly smaller probability in the case of simulated events. The size of spikes, $\langle d_{ik} \rangle$, is also systematically larger in measured events than in simulated ones. In Fig. 3 we show examples of some spiky events, both measured and simulated. The density of particles in those 'hot' regions is not very high. It exceeds the average density by a factor of $1.5 \div 2.0$. For comparison the density in the famous NA22 spike [11] was 60 times higher than the average density. But multiplicities in the analyzed central nucleus–nucleus interactions are about 50 times higher than in the NA22 pion–proton collisions. Thus, the huge combinatorial background present in high multiplicity events is probably responsible for diluting the strength of the observed signals.

TABLE II

Probabilities (in %) of the occurrence and mean values of $\langle d_{ik}\rangle$ for spikes with $d_{ik} \geq 2.5$ for the data and Monte Carlo models.

	$\delta\eta = 0.1$		$\delta\eta = 0.2$		$\delta\eta = 0.3$	
sample	$p(d_{ik} \geq 2.5)$	$\langle d_{ik}\rangle$	$p(d_{ik} \geq 2.5)$	$\langle d_{ik}\rangle$	$p(d_{ik} \geq 2.5)$	$\langle d_{ik}\rangle$
data	0.13±0.06	2.81±0.12	0.38±0.15	2.92±0.15	0.20±0.10	2.92±0.31
VENUS	0.07±0.03	2.70±0.03	0.16±0.05	2.64±0.06	0.20±0.07	2.72±0.06
FRITIOF	0.10±0.02	2.62±0.04	0.11±0.04	2.62±0.04	0.15±0.05	2.66±0.06
	$\delta\varphi = 5°$		$\delta\varphi = 10°$		$\delta\varphi = 15°$	
sample	$p(d_{ik} \geq 2.5)$	$\langle d_{ik}\rangle$	$p(d_{ik} \geq 2.5)$	$\langle d_{ik}\rangle$	$p(d_{ik} \geq 2.5)$	$\langle d_{ik}\rangle$
data	0.24±0.08	2.67±0.05	0.21±0.10	2.83±0.16	0.38±0.17	2.91±0.24
VENUS	0.10±0.03	2.66±0.03	0.12±0.04	2.73±0.08	0.21±0.08	2.72±0.07
FRITIOF	0.05±0.02	2.64±0.04	0.06±0.03	2.62±0.07	0.08±0.04	2.60±0.04

3.2. Two-dimensional $\eta - \varphi$ phase space

The search for high density regions in two-dimensional phase space corresponds to looking for jet-like (or cluster-like) phenomena. Thus, we have applied in this analysis an algorithm which uses a cone of a fixed radius to define a cluster. Such an algorithm was commonly applied to define jets in $p\overline{p}$ collisions [12], and it was proven that it indeed provides a clean separation in the $\eta - \varphi$ metric in these low multiplicity and low particle density final states. The choice of the size of a cone defined as $R \equiv \sqrt{\delta\eta^2 + \delta\varphi^2}$ is somewhat arbitrary, especially for our high density data. Therefore, we leave it as a parameter and show the results for different R_0 values. In addition we also set a cut on the minimal number of particles contained within a cone. Thus, to observe a cluster we require that particles should be confined in the cone $R \leq R_0$ and the number of particles in the cone, m, should be ≥ 5.

The non-uniform shape of the measured η distributions may affect the clustering properties of events, thus we have used a scaled variable [13] $\tilde{\eta}$ defined as

$$\tilde{\eta}(\eta) = \int_0^{\eta} \rho(\eta')d\eta' / \int_0^{6} \rho(\eta')d\eta'. \tag{7}$$

This definition ensures that $\rho(\tilde{\eta})$ is flat. Although the measured $\rho(\varphi)$ distribution is uniform, we similarly use rescaled $\tilde{\varphi}$ variables instead of φ. Thus both $\tilde{\eta}$ and $\tilde{\varphi}$ are uniformly distributed over the range $0 \div 1$ for a sample of analyzed events. The radius of the cone is redefined in $\tilde{\eta}$ and $\tilde{\varphi}$ variables. We use $\tilde{R}_0 = 0.022$, 0.047, 0.070 and 0.101 which correspond to $R_0 \approx$0.13, 0.29, 0.43 and 0.60.

In order to have some feeling how the jet algorithm works for high density data, and what degree of particle clustering in the $\tilde{\eta} - \tilde{\varphi}$ phase space we can expect, we have performed a simple event simulation in which particles were randomly selected from the uniform $\tilde{\eta}$ and $\tilde{\varphi}$ distributions. The number of particles generated per event was assumed to be equal to the measured particle multiplicity. We will refer to this simulation as SMC.

In the following we are going to investigate the degree of clustering of particles, cluster frequencies and cluster multiplicities. Since these observables are very sensitive to total event multiplicities, the comparison of experimental results with simulations is affected by the small differences observed in event multiplicities for measured and generated events [3]. Therefore, for each sample of events, we compare the results of cluster studies to the SMC results. Samples generated from the SMC have multiplicities that match those of measured or VENUS and FRITIOF events correspondingly.

The first interesting result of applying this procedure was that the fraction of particles confined in clusters (the procedure ensures that if a particle falls in the predefined cone it is excluded from the further analysis) is quite large. In Table III we present fractions of the total number of produced particles which are contained in clusters with $m \geq 5$ for four different choices of $\tilde{R}_0$. One can see that even for a quite small cone $\tilde{R}_0 = 0.047 (R_0 \approx 0.29)$ almost 50 % of produced particles forms clusters with multiplicities ≥ 5.

TABLE III

Fraction (in %) of particles contained in clusters with $\tilde{R} \leq \tilde{R}_0$ and $m \geq 5$.

$\tilde{R}_0$	sample	data	VENUS	FRITIOF
0.022		2.53 ± 0.07	2.02 ± 0.03	1.57 ± 0.03
	SMC	1.42 ± 0.05	1.77 ± 0.03	1.57 ± 0.03
0.047		49.60 ± 0.32	49.91 ± 0.17	45.73 ± 0.17
	SMC	48.09 ± 0.32	49.53 ± 0.17	45.90 ± 0.17
0.070		88.48 ± 0.43	89.24 ± 0.23	87.25 ± 0.23
	SMC	88.45 ± 0.43	89.27 ± 0.23	87.28 ± 0.23
0.101		98.44 ± 0.45	98.60 ± 0.24	98.34 ± 0.25
	SMC	98.50 ± 0.45	98.65 ± 0.24	98.38 ± 0.25

For large cones ($\tilde{R}_0 \geq 0.070$) fractions of particles contained in clusters found in measured events agree with those expected from the SMC. For smaller cones, we see slightly stronger clustering of particles in measured events than in SMC. A similar, but weaker, effect, can be seen for VENUS generated events, whereas FRITIOF simulations agree with the corresponding SMC for all choices of $\tilde{R}_0$.

In Fig. 4 the ratios of average cluster multiplicities for a given event sample to the average cluster multiplicities in corresponding SMC sample are plotted as a function of $\tilde{R}_0$. One can see that for the data, cluster multiplicities are systematically slightly larger than expected in the case of independent particle production. For the VENUS and FRITIOF samples, cluster multiplicities are consistent with those obtained from the corresponding SMC samples. Summarizing the analysis, we can conclude that we observe slightly stronger clustering of particles in the measured events than that exhibited by FRITIOF or VENUS generated events. The hypothesis of completely independent particle emission (SMC) disagrees with the measured data, indicating that a thermally equilibrated state is still not achieved in these Pb–Ag/Br central collisions.

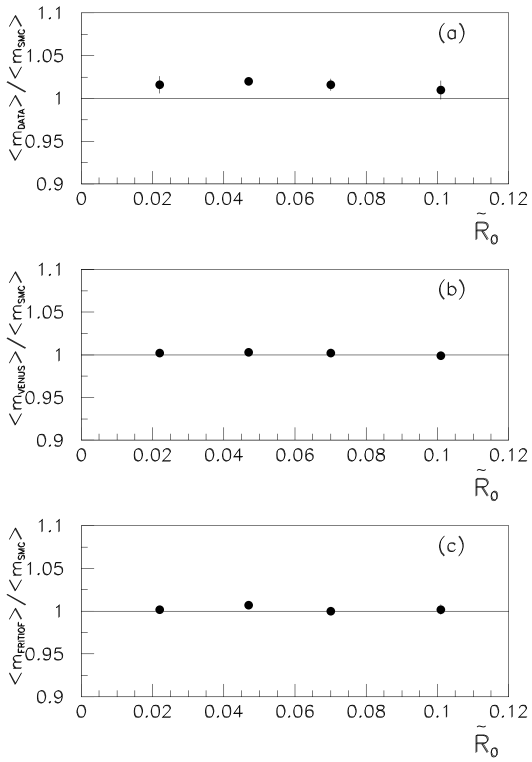

Fig. 4. Ratios of average jet multiplicities in analyzed events to those in SMC simulated events for the data (a), VENUS events (b) and FRITIOF events (c).

The fact that the results obtained from model simulations agree with SMC and that only small deviations from SMC are observed in the measured events, shows again the dominance of combinatorial background in the high multiplicity events.

4. Factorial moments in individual events

The preliminary results of the analysis of factorial moments applied to single collision events were presented by us in [2, 14]. Here, we show the results from larger sample of central Pb–Ag/Br collisions.

A decade ago it was shown [15] that factorial moments calculated for a single high multiplicity cosmic ray interaction increase with decreasing size of the η bin, thus indicating the presence of dynamical, intermittent-type fluctuations in this event. It is interesting to see whether this property is typical for every high multiplicity event. If it is not , the analysis of factorial moments could be used as a tool for selecting events with strong dynamical fluctuations. Having now a set of high multiplicity Pb–Ag/Br collisions, we can check the above suppositions.

For a given event we define the factorial moment of the order q as [17]:

$$F_q^{ev}(M) = S\frac{f_q^{ev}}{B} = S\frac{\frac{1}{M}\sum_{i=1}^{M} n_{ik}(n_{ik}-1)...(n_{ik}-q+1)}{\frac{1}{N_{ev}^q}\frac{1}{M}\sum_{i=1}^{M} N_i(N_i-1)...(N_i-q+1)}, \tag{8}$$

where n_{ik} denotes the number of particles in the i-th phase space cell of the k-th event. The number of events and the number of partitions of the phase space region into smaller cells are denoted by N_{ev} and M respectively. $N_i = \sum_{k=1}^{N_{ev}} n_{ik}$. As is seen from Eq. (8) we have taken for the normalization, B, the average over all events in the analyzed data set (see [3]) in order to reduce statistical errors. Therefore, a scaling factor, S, was introduced to account for the difference between event multiplicity and the average multiplicity of the sample:

$$S = \frac{\langle f_q^{ev}(M=1)\rangle}{f_q^{ev}(M=1)}, \tag{9}$$

where brackets, $\langle\ \rangle$, denote averaging over events. The analysis was performed in $\tilde{\eta}$ and $\tilde{\varphi}$ bins and in two-dimensional $\tilde{\eta}$ - $\tilde{\varphi}$ cells.

It is not obvious how to calculate the uncertainties of factorial moments measured in single events. In our previous analysis in η and φ variables [2], the uncertainties of $F_q^{ev}(M)$ were estimated from the spread of moments calculated for slightly different choices of the η range (see [2] for more details). The resultant uncertainties were smaller than 15 %. We expect the same uncertainties for the moments calculated in scaled $\tilde{\eta}$ and $\tilde{\varphi}$ variables. In the following, since we are only interested in any increase of the factorial moments with decreasing size of the phase space cell, we show the calculated moments without the uncertainties. The observation of such an increase signals the presence of non-statistical fluctuations.

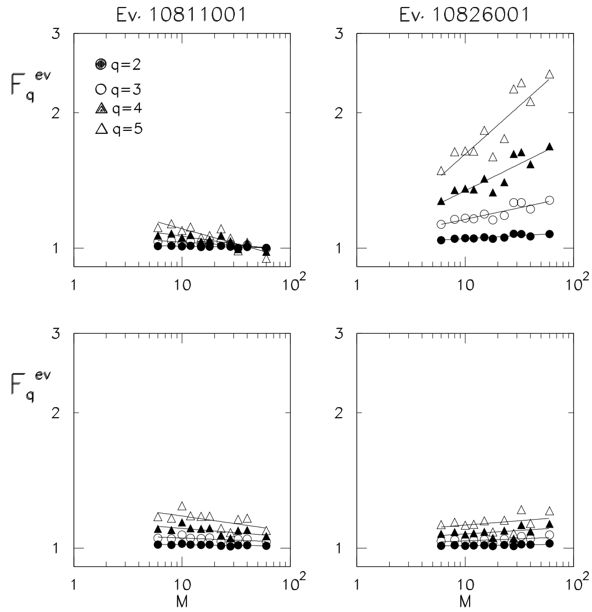

Fig. 5a. Log-log plots of the factorial moments F_q^{ev} vs the number M of cells calculated for the two Pb–Ag/Br events in the one-dimensional $\tilde{\eta}$ (upper plots) and $\tilde{\varphi}$ (lower plots) bins. Lines show the fits to power law functions.

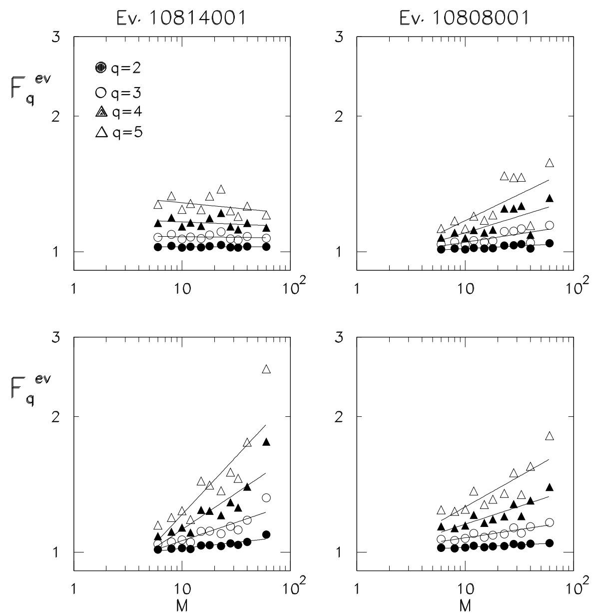

Fig. 5b. The same as in Fig. 5a but for another two Pb–Ag/Br events.

From event-to-event we observe quite different patterns of dynamical fluctuations. In some events an increase of the factorial moments with decreasing bin size is seen in both $\tilde{\eta}$ and $\tilde{\varphi}$ variables. On the other hand there are also some events in which there is no evidence for the presence of dynamical fluctuations. In some events we even observe decreasing factorial moments for small bin widths. The behavior of the factorial moments for some selected events is shown in Figs 5a and 5b. One can clearly see different fluctuation patterns in the various events.

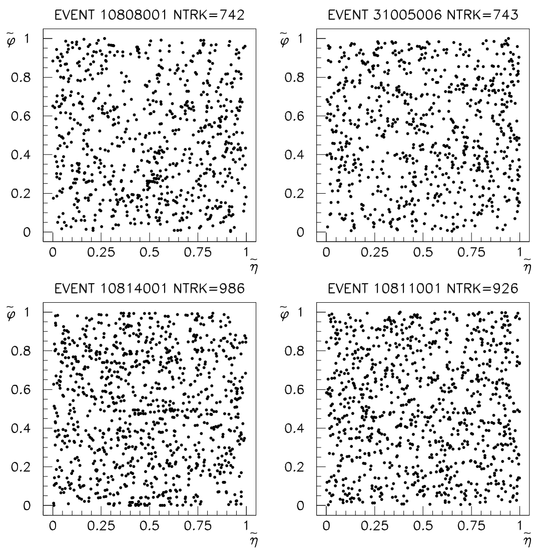

Fig. 6. $\tilde{\eta} - \tilde{\varphi}$ scatter plots for the two events with strong dynamical fluctuations (left-side plots) and the two events without dynamical fluctuations (right-side plots).

The above analysis indicates that the factorial moments method could be used to select those events with strong dynamical fluctuations. To illustrate the efficiency of this method we compare in Fig. 6 the $\tilde{\eta} - \tilde{\varphi}$ scatter plots for the two events with strong fluctuations (left-side plots) to scatter plots for the two events which do not exhibit dynamical fluctuations (right-side plots). The dependencies of the two-dimensional factorial moments on the number of $\tilde{\eta}$ - $\tilde{\varphi}$ cells for the same events are shown in Fig. 7. Visual inspection of Fig. 6 does not allow us to differentiate between events with and without evidence for dynamical fluctuations. Yet, by using the factorial moments (see Fig. 7) it is easily possible. Consequently, the measured intermittency patterns can be used as a preliminary selection of events. Then more advanced triggering may be applied, based *e.g.* on the unusual particle ratios, enhancement of the particle production in certain kinematical regions, *etc.*

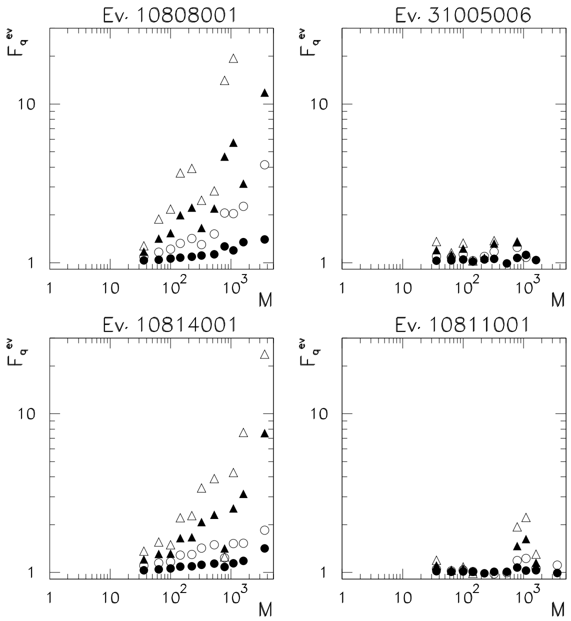

Fig. 7. Log-log plots of the factorial moments F_q^{ev} vs the number M of cells calculated for the same events as shown in Fig. 6 in the two-dimensional $\tilde{\eta}$–$\tilde{\varphi}$ cells.

5. Summary

We have presented different methods of analyzing individual nucleus–nucleus interactions. These methods have been applied to study, on an event-by-event basis, high multiplicity collisions of Pb(158 GeV/nucleon) with the Ag/Br targets of nuclear emulsion from the EMU13 experiment. The 4π measurements of particles produced in these collisions ensures that the results on single event properties are not distorted by acceptance cuts.

The global characterization of particle pseudorapidity distributions has not revealed the presence of anomalous events. The variable Φ_η was found to be consistent with the expectations from VENUS and FRITIOF simulations. The analysis of the roughness of η distributions showed no significant deviations of the single event spectra from the distribution averaged over the sample of all events. Clearly the analysis of global event properties requires large event samples and our statistics may be insufficient to detect small deviations in the distribution of global observables from the expectations based on a conventional description of nucleus–nucleus collisions.

The search for high density regions in the one-dimensional η and φ distributions showed the rare occurrence of small phase space domains with densities that exceeded, by a factor of $1.5 \div 2$, the average density. Similar densely populated regions are also seen in Monte Carlo simulations, but with a slightly smaller probability. Cluster-like objects were identified in the two-dimensional $\eta - \varphi$ phase space by using the cone algorithm. The analysis revealed a slightly stronger clustering of particles in the measured events than in the VENUS or FRITIOF generated events. We have also observed deviations from the scenario of completely independent particle emission in the analysis of clusters with small angular separation.

A systematic study of particle density fluctuations at all scales was performed by means of the factorial moments method. In single collision events we observed different patterns of dynamical fluctuations. Therefore the method can be used as an effective tool for selecting interesting events, those exhibiting large dynamical fluctuations.

The analysis presented here indicates that the effects observed in high multiplicity events are dominated by a large combinatorial background. The search for large event anomalies in future heavy ion experiments can be performed with the help of known methods, such as those discussed in this paper. On the other hand, the detection of small effects will be extremely difficult. It is, therefore, important to perform further tests of the sensitivities of various methods and to put more effort into the development of new techniques especially tuned to reveal small deviations from the expectations based on a conventional physics model of nucleus–nucleus collisions.

This work was partially supported in Poland by the State Committee for Scientific Research Grant 2P03B18409and MSC Fund II PAA/NSF-96-256, in the U.S. by the National Science Foundation (Grant PHY-513997 at LSU) and Department of Energy (DOE-FG02-89ER40528 at Minnesota).

REFERENCES

[1] H.Satz, *Nucl. Phys.* **A566**, 1c (1994); J.P.Blaizot, *Nucl. Phys.* **A566**, 333c (1994); F.Karsch, *Nucl. Phys.* **A590**, 367c (1995).

[2] B.Wosiek and the KLMM Collab., Proc.XXV Int. Symp. on Multiparticle Dynamics, Stara Lesna, 1995, World Sci., 1996, p. 271.

[3] A. Dąbrowska *et al.*, (KLM Collab.), accepted for publication in *Nucl. Phys.* **A**.

[4] H. Pi, *Comput. Phys. Commun.* **71**, 173 (1992).

[5] K. Werner, *Phys. Rep.* **232**, 87 (1995).

[6] G. Roland and the NA49 Collab., Proc. of the Quark Matter'97 Conference, Tsukuba, Japan; to be published in *Nucl. Phys.* **A**.

[7] P. Deines-Jones *et al.*, (KLM Collab.), *Phys. Rev.* **C53**, 3044 (1996).

[8] J.P. Blaizot, A. Krzywicki, *Phys. Rev.* **D46**, 246 (1992); K. Rajagopal, F. Wilczek, *Nucl. Phys.* **B399**, 395 (1993); J. Randrup, R.L. Thews, *Phys. Rev.* **D55**, 6900 (1997).

[9] B. Wyslouch and the WA98 Collab. Warsaw Conf.(1996).

[10] M. Gaździcki, St. Mrówczyński, *Z. Phys.* **C54**, 127 (1992).

[11] M. Adamus *et al.*, (NA22 Collab.), *Phys. Lett.* **B185**, 200 (1987).

[12] F. Abe *et al.*, (CDF Collab.), *Phys. Rev.* **D45**, 1448 (1992).

[13] A. Białas, M. Gaździcki, *Phys. Lett.* **B252**, 483 (1990).

[14] B. Wosiek, *Acta Phys. Slovaca* **46**, 531 (1996).

[15] A. Białas, R. Peschanski, *Nucl. Phys.* **B308**, 857 (1988).

[16] A. Białas, R. Peschanski, *Nucl. Phys.* **B273**, 703 (1986).

[17] K. Kadija, P. Seyboth, *Z. Phys.* **C61**, 465 (1994).